Precise $\overline{\text{MS}}$ light-quark masses from lattice QCD in the RI/SMOM scheme

Martin Gorbahn

Technische Universität München, Institute for Advanced Study, Arcisstraße 21,D-80333 München, Germany and
Technische Universität München, Excellence Cluster "Universe",
Boltzmannstraße 2, D-85748 Garching, Germany**

Sebastian Jäger

University of Sussex, Department of Physics and Astronomy, Falmer, Brighton BN1 9QH, UK†
(Dated: April, 2010)

We compute the conversion factors needed to obtain the $\overline{\text{MS}}$ and RGI up, down, and strange-quark masses at next-to-next-to-leading order from the corresponding parameters renormalized in the recently proposed RI/SMOM and RI/SMOM$_{\gamma_\mu}$ renormalization schemes. This is important for obtaining the $\overline{\text{MS}}$ masses with the best possible precision from numerical lattice-QCD simulations, because the customary RI$^{(\prime)}$/MOM scheme is afflicted with large irreducible uncertainties both on the lattice and in perturbation theory. We find that the smallness of the known one-loop matching coefficients is accompanied by even smaller two-loop contributions. From a study of residual scale dependences, we estimate the resulting perturbative uncertainty on the light-quark masses to be about 2% in the RI/SMOM scheme and about 3% in the RI/SMOM$_{\gamma_\mu}$ scheme. Our conversion factors are given in fully analytic form, for general covariant gauge and renormalization point. We provide expressions for the associated anomalous dimensions.

Lattice QCD has, in recent years, seen important progress on several fronts: there exist lattice regularizations preserving exact chiral symmetry in the limit of vanishing quark masses, while algorithmic and technological advances have put lattices fine enough to simulate physical light-quark masses within reach. As a result, nonperturbative results in the physics of light quarks with a precision of a few percent or better become achievable with current or upcoming simulations [1]. These include the masses of the light quarks, as well as hadronic matrix elements such as B_K, figuring prominently in the unitarity-triangle analysis. At such high precision, choices of renormalization scheme and associated perturbative higher-order effects become an important source of uncertainty. Two standard methods have emerged: the use of momentum-space subtraction schemes that can be nonperturbatively implemented on a lattice [2] and the Schrödinger-functional method [3], where so-called renormalization-group-invariant (RGI) masses and matrix elements are obtained via a direct implementation of the renormalization group on the lattice. Within the former approach, parameters need a further conversion to purely perturbative schemes such as $\overline{\text{MS}}$ [4], where short-distance QCD and new-physics effects are best tractable.

It has recently been realized that the standard RI$^{(\prime)}$/MOM prescription suffers from a strong sensitivity to IR effects [5], which has become the dominant source of uncertainty on the lattice. This is paralleled by unusually large higher-order terms in the perturbative conversion factors [6]. A modified scheme with much better IR behaviour has been recently proposed and called RI/SMOM [7]. In this work, we study the renormalization of the pseudoscalar (non-singlet) density, which by virtue of chiral symmetries is related to the renormalization of the quark mass, and obtain the next-to-next-to-leading-order (NNLO, two-loop) conversion factor allowing to obtain $\overline{\text{MS}}$ light quark masses from their counterparts renormalized in the RI/SMOM scheme, or its variant RI/SMOM$_{\gamma_\mu}$, as 'measured' on the lattice. We find much smaller perturbative corrections than in the RI$^{(\prime)}$/MOM case, extending one-loop findings in [7] and implying percent-level uncertainties on the $\overline{\text{MS}}$ masses.

RI′/MOM, RI/SMOM, AND RI/SMOM$_{\gamma_\mu}$

In the RI′/MOM renormalization scheme for the quark field and mass, two conditions [2]

$$\lim_{m_R \to 0} \frac{1}{12\, p^2} \text{tr}[S_R^{-1}(p)\not{p}]\Big|_{p^2=-\mu^2} = -1, \qquad (1)$$

$$\lim_{m_R \to 0} \frac{1}{12\, m_R} \text{tr}[S_R^{-1}(p)]\Big|_{p^2=-\mu^2} = 1, \qquad (2)$$

are imposed on the inverse quark propagator $S_R^{-1} = Z_q^{-1} S_B^{-1}$. The bare quark propagator S_B is defined through (our notation closely follows [7])

$$-i\, S_B(p) = \int \mathrm{d}^4 x\, e^{ipx} \langle T(\psi_B(x)\bar\psi_B(0))\rangle, \qquad (3)$$

and the traces are over colour and Dirac indices. (1) and (2) determine the renormalization constants Z_q and Z_m relating bare and renormalized field and mass, $\psi_R = Z_q^{1/2}\psi_B$ and $m_R = Z_m m_B$. Both renormalization constants depend implicitly on the regulator (lattice, dimensional regularization, etc.) and on the gauge coupling and the gauge parameter. A virtue of the RI′/MOM scheme is that it can be implemented nonperturbatively on the lattice as well as in dimensionally regularized continuum perturbation theory. The RI′/MOM field and

mass can then be converted perturbatively to the $\overline{\text{MS}}$ scheme via $\psi_R^{\overline{\text{MS}}} = (Z_q^{\overline{\text{MS}}}/Z_q^{\text{RI}'/\text{MOM}})^{1/2}\psi_R^{\text{RI}'/\text{MOM}}$ and $m_R^{\overline{\text{MS}}} = Z_m^{\overline{\text{MS}}}/Z_m^{\text{RI}'/\text{MOM}}\,m_R^{\text{RI}'/\text{MOM}}$, where all renormalization constants have to be computed with the same (but otherwise arbitrary) regulator. Both conversion factors are known to three-loop accuracy [6, 8]. However, the perturbation series does not converge well, and this constitutes a drawback of using the RI$'$/MOM scheme for extracting light-quark masses from lattice simulations. Another issue is the influence of non-perturbative long-distance physics. This is most clearly seen by considering (non-singlet) axial-current Ward identities such as

$$q_\mu \Lambda_{A,B}^\mu(p,p') =$$
$$S_B^{-1}(p')\gamma_5 + \gamma_5 S_B^{-1}(p) + i(m_{u,B}+m_{s,B})\Lambda_{P,B}(p,p'), \quad (4)$$

where $q \equiv p - p'$, and the bare vertex functions $\Lambda_{A,B}^\mu$ for the axial current and $\Lambda_{P,B}$ for the pseudoscalar density are defined through

$$S_B(p')\Lambda_{A,B}^\mu(p,p')S_B(p) \quad (5)$$
$$= \int d^4x\,d^4y\,e^{ip'x}e^{-ipy}\,\langle T([i\bar{u}_B\gamma^\mu\gamma_5 s_B](0)\,u_B(x)\,\bar{s}_B(y))\rangle,$$

$$S_B(p')\Lambda_{P,B}(p,p')S_B(p)$$
$$= \int d^4x\,d^4y\,e^{ip'x}e^{-ipy}\,\langle T([i\bar{u}_B\gamma_5 s_B](0)\,u_B(x)\,\bar{s}_B(y))\rangle. \quad (6)$$

(4) holds for a regulator which respects chiral symmetry (in the limit $m_B \to 0$). This is the case for certain lattice regularizations and for dimensional regularization with anticommuting γ_5. (The use of anticommuting γ_5 is unproblematic here as (4) and the formulae below do not involve closed traces containing odd powers of γ_5.) To preserve (4) under renormalization, the axial current must not be renormalized, and the renormalization constant Z_P of the pseudoscalar density must satisfy $Z_P = Z_m^{-1}$, where Z_P can be fixed by imposing the condition

$$\lambda_R(p^2,p'^2,q^2) = Z_q^{-1}Z_P\,\lambda_B(p^2,p'^2,q^2)$$
$$\equiv Z_q^{-1}Z_P\,\text{tr}[\Lambda_{P,B}(p,p')\gamma_5] \overset{!}{=} 12 \quad (7)$$

at a suitable subtraction point. The choice $p^2 = p'^2 = -\mu^2$, $q^2 = 0$ corresponds to (2). But at $q^2 = 0$, $\Lambda_{P,B}(p,p')$ receives contributions from the kaon (pseudo-Goldstone) pole, which diverge in the chiral limit $m_R \to 0$ [2], and is sensitive to condensate effects suppressed only by $(\Lambda_{\text{QCD}}/\mu)^2$ [5]. In [7], a modified renormalization scheme, termed RI/SMOM, was proposed, which is less sensitive to these effects. In that scheme, (7) is imposed at the symmetric point $p^2 = p'^2 = q^2 = -\mu^2$. Following [7], we will consider a more general kinematic configuration $p^2 = p'^2 = -\mu^2$, $q^2 = -\omega\mu^2$ below, and define conversion factors

$$C_q^{\text{RI/SMOM}} = C_q^{\text{RI}'/\text{MOM}} = \frac{Z_q^{\overline{\text{MS}}}}{Z_q^{\text{RI}'/\text{MOM}}} = \frac{12\,\mu^2 Z_q^{\overline{\text{MS}}}}{\sigma_B(-\mu^2)}, \quad (8)$$

$$C_m^{\text{RI/SMOM}}(\omega) = \frac{Z_m^{\overline{\text{MS}}}}{Z_m^{\text{RI/SMOM}}(\omega)} = \frac{Z_m^{\overline{\text{MS}}}\sigma_B(-\mu^2)}{\mu^2\,\lambda_B(-\mu^2,-\mu^2,-\omega\mu^2)}, \quad (9)$$

where $\sigma_B(p^2) \equiv \text{tr}[S_B^{-1}(p)\slashed{p}]$. The right-most expression in (9) has a straightforward perturbation expansion. Moreover, in [7] a variant scheme RI/SMOM$_{\gamma_\mu}$ was introduced where the field-renormalization condition (1) is replaced by the requirement

$$\tilde{\lambda}_R(p^2,p'^2,q^2) = Z_q^{-1}\,\tilde{\lambda}_B(p^2,p'^2,q^2)$$
$$\equiv Z_q^{-1}\,\text{tr}[\Lambda_{A,B}^\mu(p,p')\gamma_5\gamma_\mu] \overset{!}{=} 48, \quad (10)$$

which implies conversion factors

$$C_q^{\text{RI/SMOM}_{\gamma_\mu}}(\omega) = \frac{48\,Z_q^{\overline{\text{MS}}}}{\tilde{\lambda}_B(-\mu^2,-\mu^2,-\omega\mu^2)}, \quad (11)$$

$$C_m^{\text{RI/SMOM}_{\gamma_\mu}}(\omega,\omega') = \frac{Z_m^{\overline{\text{MS}}}\,\tilde{\lambda}_B(-\mu^2,-\mu^2,-\omega'\mu^2)}{4\,\lambda_B(-\mu^2,-\mu^2,-\omega\mu^2)}. \quad (12)$$

The schemes for field and mass are converted as

$$\psi^{\overline{\text{MS}}} = (C_q^X)^{1/2}\,\psi^X, \quad m^{\overline{\text{MS}}} = C_m^X\,m^X, \quad (13)$$

where $X = \text{RI/SMOM}$ or $\text{RI/SMOM}_{\gamma_\mu}$.

We note that C_q^X and C_m^X depend on $\ln\mu^2/\nu^2 \equiv \ln r$, where ν is the dimensional renormalization scale, and implicitly on ν through the scale dependence of α_s and the gauge parameter ξ. Setting $\mu \equiv \nu$ allows relating the anomalous dimensions in the RI/SMOM schemes to those in the $\overline{\text{MS}}$ scheme [9–12] according to

$$\gamma_m^X = \gamma_m^{\overline{\text{MS}}} - \left[\frac{\beta(\alpha_s)}{4}\frac{\partial}{\partial\left(\frac{\alpha_s}{4\pi}\right)} + \delta(\alpha_s,\xi)\frac{\partial}{\partial\xi}\right]\ln C_m^X\Big|_{r=1}, \quad (14)$$

$$\gamma_q^X = \gamma_q^{\overline{\text{MS}}} - \left[\frac{\beta(\alpha_s)}{4}\frac{\partial}{\partial\left(\frac{\alpha_s}{4\pi}\right)} + \delta(\alpha_s,\xi)\frac{\partial}{\partial\xi}\right]\ln C_q^X\Big|_{r=1}. \quad (15)$$

Here we use the definitions (which conform to [7])

$$\gamma_m^Y m^Y = \mu^2\frac{d}{d\mu^2}m^Y, \quad \gamma_q^Y\psi^Y = 2\mu^2\frac{d}{d\mu^2}\psi^Y, \quad (16)$$

$$\beta(\alpha_s) = \mu^2\frac{d}{d\mu^2}\frac{\alpha_s}{\pi}, \quad \delta(\alpha_s,\xi) = \mu^2\frac{d}{d\mu^2}\xi, \quad (17)$$

with $Y = \overline{\text{MS}}$ or RI/SMOM or RI/SMOM$_{\gamma_\mu}$.

NNLO COMPUTATION

We now compute the conversion factors to $\mathcal{O}(\alpha_s^2)$ in dimensional regularization ($d = 4 - 2\epsilon$). Let us denote

$$\sigma = -4N_c p^2 + \sigma^{(1)} + \sigma^{(2)} + \mathcal{O}(\alpha_s^3), \quad (18)$$
$$\lambda = 4N_c + \lambda^{(1)} + \lambda^{(2)} + \mathcal{O}(\alpha_s^3), \quad (19)$$
$$\tilde{\lambda} = 4\,d\,N_c + \tilde{\lambda}^{(1)} + \tilde{\lambda}^{(2)} + \mathcal{O}(\alpha_s^3), \quad (20)$$

where the superscripts denote the loop order. $\sigma^{(1)}$, $\lambda^{(1)}$, and $\tilde{\lambda}^{(1)}$ have been evaluated in [7]. For the present computation, we also need their $\mathcal{O}(\epsilon)$ parts, which will affect

the $\mathcal{O}(\alpha_s^2)$ results for C_q and C_m. Taking the traces and employing partial fractions, we obtain

$$\sigma_B^{(1)}(p^2) = 4N_c C_F \, (-p^2)^{1-\epsilon} \, \frac{\alpha_s}{4\pi} \left(\nu^2 e^{\gamma_E}\right)^{\epsilon}$$

$$\times \left\{ \frac{d+\xi-3}{2} g(1,1) + \frac{1-\xi}{2} g(2,1) \right\}, \tag{21}$$

$$\lambda_B^{(1)}(p^2, p'^2, q^2) = 4N_c C_F \frac{\alpha_s}{4\pi} \frac{d-(1-\xi)}{2} \tag{22}$$

$$\times \left\{ q^2 j(1,1,1; p^2, p'^2, q^2) + g(1,1)e^{\gamma_E \epsilon} \left[\left(\frac{\nu^2}{-p^2}\right)^{\epsilon} + \left(\frac{\nu^2}{-p'^2}\right)^{\epsilon} \right] \right\},$$

$$\tilde{\lambda}_B^{(1)}(p^2, p'^2, q^2) = 2N_c C_F \frac{\alpha_s}{4\pi} \tag{23}$$

$$\times \left\{ \left[(d-2)^2 q^2 - (d-2)(1-\xi)\left(p^2+p'^2\right) \right] j(1,1,1; p^2, p'^2, q^2) \right.$$

$$-2\,(d-2)(1-\xi)\,g(1,1)e^{\gamma_E \epsilon}\left(\frac{\nu^2}{-q^2}\right)^{\epsilon} + \left[2\,(1-\xi)g(1,2) \right.$$

$$\left. + \left((d-2)^2+(d-4)(1-\xi)\right)g(1,1)\right]e^{\gamma_E \epsilon}\left[\left(\frac{\nu^2}{-p^2}\right)^{\epsilon}+\left(\frac{\nu^2}{-p'^2}\right)^{\epsilon}\right]\right\},$$

where γ_E is the Euler-Mascheroni constant, ν the dimensional renormalization scale and

$$g(\nu_1, \nu_2) = \frac{\Gamma(\nu_1+\nu_2+\epsilon-2)\Gamma(2-\epsilon-\nu_1)\Gamma(2-\epsilon-\nu_2)}{\Gamma(\nu_1)\Gamma(\nu_2)\Gamma(4-\nu_1-\nu_2-2\epsilon)}. \tag{24}$$

The function j results from a massless triangle, via

$$j(\nu_1, \nu_2, \nu_3; p_1^2, p_2^2, p_3^2) \equiv \left(\frac{i}{16\pi^2}\right)^{-1}\left(\frac{\nu^2}{4\pi}e^{\gamma}\right)^{\epsilon}$$

$$\times \int \frac{d^d k}{(2\pi)^d} \frac{1}{[-k^2]^{\nu_3}[-(k+p_1)^2]^{\nu_2}[-(k-p_2)^2]^{\nu_1}}, \tag{25}$$

with $p_3 = -(p_1+p_2)$. Several cases have been evaluated in [13] (our j is essentially their J), in particular

$$j(1,1,1; p_1^2, p_2^2, p_3^2) = \tag{26}$$

$$\left(\frac{\nu^2}{-p_3^2}e^{\gamma_E}\right)^{\epsilon} \frac{\Gamma(1+\epsilon)}{p_3^2}\left(\Phi^{(1)}(x,y)+\epsilon\Psi^{(1)}(x,y)+\mathcal{O}(\epsilon^2)\right),$$

where $x = p_1^2/p_3^2$ and $y = p_2^2/p_3^2$. The functions $\Phi^{(1)}(x,y)$ and $\Psi^{(1)}(x,y)$ have been given in [13] in terms of polylogarithms up to second and third order, respectively.

At the two-loop level, the relevant diagrams are shown in Figure 1. They can be represented in terms of three master "topologies" (Figure 2), which may be called "propagator", "ladder", and "non-planar", with their propagators raised to general integer powers. For the latter two topologies, irreducible numerators occur. The set can be reduced by standard reduction techniques and a systematic application integration-by-parts (IBP) identities. For this we employ the program FIRE [15], a public implementation of Laporta's algorithm [16] and the method of S-bases [17]. A subtle apsect of the IBP reduction is the occurence of quadratic and simple poles in ϵ in the coefficients of the resulting integrals. In a
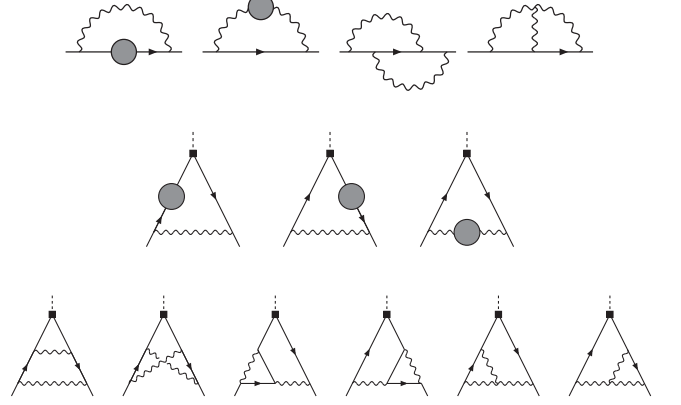

FIG. 1. Two-loop propagator and vertex diagrams. The grey blobs indicate a sum over all one-loop corrections to a propagator, the black boxes an insertion of a fermion bilinear
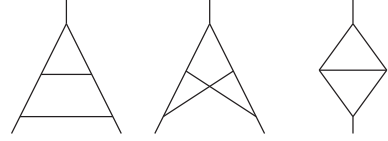

FIG. 2. Basic three- and two-point topologies: ladder, nonplanar, propagator (from left to right)

two-loop computation, this leads to poles of up to fourth order. On the other hand, the Feynman diagrams have poles of at most second order, entirely of ultraviolet origin. The spurious third- and fourth-order poles cancel, which constitutes a check of the computation, but they also imply a possible dependence on terms up to $\mathcal{O}(\epsilon^3)$ in the ϵ expansion of the master integrals remaining after the reduction. In practice, we find that only known master integrals [13, 14] are needed, except for the unknown $\mathcal{O}(\epsilon^2)$ part of $j(1,1,2+\epsilon)$. Denoting

$$j(1,1,2+\epsilon; p_1^2, p_2^2, p_3^2) = \left(\frac{\nu^2}{-p_3^2}e^{\gamma}\right)^{\epsilon}\Gamma(1+\epsilon)(-p_3^2)^{-2-\epsilon}$$

$$\times \frac{1}{2(1+\epsilon)xy}\left(-\frac{1}{\epsilon}+2\ln(xy)+\epsilon\left[\frac{\pi^2}{6}-2\left(\ln^2 x+\ln^2 y\right)\right.\right.$$

$$\left.\left. -\ln x \ln y -3(1-x-y)\Phi^{(1)}(x,y)\right]+\epsilon^2\,\Xi^{(1)}(x,y)+\mathcal{O}(\epsilon^3)\right),$$

we find that

$$\Xi^{(1)}(x,x) = \frac{1}{2}\,\Omega^{(2)}(x,x)-\Omega^{(2)}\left(1,\frac{1}{x}\right)-(3-6x)\Psi^{(1)}(x,x)$$

$$+\frac{11}{3}\ln^3 x +14\,\zeta(3)+\ln x\left((3-6x)\Phi^{(1)}(x,x)-\frac{2}{3}\pi^2\right), \tag{27}$$

$$\Xi^{(1)}\left(1,\frac{1}{x}\right) = -\frac{1}{2}\Omega^{(2)}(x,x)+3\,\Psi^{(1)}(x,x)$$

$$-\frac{4}{3}\ln^3 x +14\,\zeta(3)+\ln x\left(\frac{\pi^2}{3}+\frac{9}{2}\Phi^{(1)}(x,x)\right). \tag{28}$$

The function $\Omega^{(2)}$ arises in evaluating ladder master integrals [13, 14] and is given there in terms of polyloga- rithms. Combining all terms and $\overline{\text{MS}}$-renormalizing the gauge coupling and gauge parameter, we obtain

$$
\begin{aligned}
C_m^{\text{RI/SMOM}}(\omega) = {}& 1 + \frac{\alpha_s}{4\pi}\,C_F\left(\frac{3+\xi}{2}\,\Phi^{(1)}\!\left(\frac{1}{\omega},\frac{1}{\omega}\right) - 4 - \xi + 3\ln r\right) + \left(\frac{\alpha_s}{4\pi}\right)^2 C_F\left\{N_c\left(-\frac{2513}{48} - \frac{3\,\xi}{2} - \frac{\xi^2}{4} + 12\,\zeta(3)\right.\right.\\
& + \frac{307+6\,\xi^2}{12}\ln r - \frac{13}{4}\ln^2 r + \left[\frac{301}{24} + \frac{3\,\xi}{4} - \frac{\xi^2}{8} - \frac{13+\xi^2}{4}\ln r - \frac{7+3\,\xi}{4}\ln\omega\right]\Phi^{(1)}\!\left(\frac{1}{\omega},\frac{1}{\omega}\right) + \frac{9+6\,\xi+\xi^2}{8}\Phi^{(1)}\!\left(\frac{1}{\omega},\frac{1}{\omega}\right)^2\\
& \left. + \omega\,\Phi^{(2)}(1,\omega) - \frac{3+\xi}{2}\Phi^{(2)}\!\left(\frac{1}{\omega},\frac{1}{\omega}\right)\right) + n_f\left(\frac{83}{12} + \left[\ln r - \frac{5}{3}\right]\Phi^{(1)}\!\left(\frac{1}{\omega},\frac{1}{\omega}\right) - \frac{13}{3}\ln r + \ln^2 r\right)\\
& + \frac{1}{N_c}\left(-\frac{19}{16} - 2\,\xi - \frac{\xi^2}{2} + \left[\frac{7}{2} + \xi + \frac{\xi^2}{2} - \frac{9+3\,\xi}{4}\ln r + \frac{5+3\,\xi}{4}\ln\omega\right]\Phi^{(1)}\!\left(\frac{1}{\omega},\frac{1}{\omega}\right) + \frac{21+6\,\xi}{4}\ln r - \frac{9}{4}\ln^2 r\right.\\
& \left.\left. + \frac{1+\xi}{2}\Phi^{(2)}\!\left(\frac{1}{\omega},\frac{1}{\omega}\right) + \frac{1}{2}\Omega^{(2)}\!\left(\frac{1}{\omega},\frac{1}{\omega}\right) - \Omega^{(2)}(1,\omega) - \left[\frac{5}{8} + \frac{3\,\xi}{4} + \frac{\xi^2}{8} + \frac{1}{\omega}\right]\Phi^{(1)}\!\left(\frac{1}{\omega},\frac{1}{\omega}\right)^2\right)\right\} + \mathcal{O}\left(\alpha_s^3\right),
\end{aligned}
\tag{29}
$$

$$
\begin{aligned}
C_q^{\text{RI/SMOM}_{\gamma_\mu}}(\omega) = {}& 1 + \frac{\alpha_s}{4\pi}\,C_F\left(1 - \frac{3\,\xi}{2} + \xi\ln r - \frac{1-\xi}{2}\ln\omega + \frac{\omega-1+\xi}{2\,\omega}\Phi^{(1)}\!\left(\frac{1}{\omega},\frac{1}{\omega}\right)\right)\\
& + \left(\frac{\alpha_s}{4\pi}\right)^2 C_F\left\{N_c\left(-\frac{71}{144} - \frac{35\,\xi}{4} - \frac{5\,\xi^2}{8} - \frac{3-9\,\xi}{2}\zeta(3) + \left[\frac{11}{6} + \frac{19\,\xi}{4} + \frac{\xi^2}{4} + \left(\frac{11}{6} - \xi\right)\ln\omega\right]\ln r - \frac{3\,\xi}{4}\ln^2 r\right.\right.\\
& + \left[\frac{223\,\omega-259}{72\,\omega} + \frac{\omega+20}{8\,\omega}\xi - \frac{\xi^2}{8\,\omega} + \frac{22(1-\omega)+(3\,\omega-12)\xi}{12\,\omega}\ln r + \frac{1+(\omega-2)\xi+\xi^2}{4\,\omega}\ln\omega\right]\Phi^{(1)}\!\left(\frac{1}{\omega},\frac{1}{\omega}\right)\\
& - \frac{259-180\,\xi+9\,\xi^2}{72}\ln\omega + \frac{(1-\xi)^2}{8}\ln^2\omega + \frac{(1-\omega-\xi)^2}{8\,\omega^2}\Phi^{(1)}\!\left(\frac{1}{\omega},\frac{1}{\omega}\right)^2 + \frac{1-\xi}{4}\Omega^{(2)}(1,\omega) - \frac{3-\xi}{8}\Omega^{(2)}\!\left(\frac{1}{\omega},\frac{1}{\omega}\right)\\
& \left. + \frac{\omega}{2}\Phi^{(2)}(1,\omega) + \frac{3-2\,\omega-\xi}{2\,\omega}\Phi^{(2)}\!\left(\frac{1}{\omega},\frac{1}{\omega}\right)\right) + n_f\left(\frac{5}{36} - \frac{1+\ln\omega}{3}\ln r + \frac{5}{9}\ln\omega + \frac{(1-\omega)(5-3\ln r)}{9\,\omega}\Phi^{(1)}\!\left(\frac{1}{\omega},\frac{1}{\omega}\right)\right)\\
& + \frac{1}{N_c}\left(\frac{1}{16} + \frac{\xi}{2} - \frac{7\xi^2}{8} + 3\,(1-\xi)\,\zeta(3) - \frac{\xi^2}{4}\ln^2 r + \frac{1-3\,\xi+2\,\xi^2}{4}\ln\omega + \left[\frac{3-2\,\xi+3\,\xi^2}{4} + \frac{\xi(1-\xi)}{4}\ln\omega\right]\ln r\right.\\
& - \frac{(1-\xi)^2}{8}\ln^2\omega + \left[\frac{13}{8} + \frac{1}{4\,\omega} - \frac{6+\omega}{8\,\omega}\xi + \frac{\xi^2}{2\,\omega} + \frac{\xi(1-\omega-\xi)}{4\,\omega}\ln r - \frac{1+\omega+\xi(\omega-2)+\xi^2}{4\,\omega}\ln\omega\right]\Phi^{(1)}\!\left(\frac{1}{\omega},\frac{1}{\omega}\right)\\
& \left.\left. - \frac{1+\omega\,(2-\omega)-2\,\xi(1-\omega)+\xi^2}{8\,\omega^2}\Phi^{(1)}\!\left(\frac{1}{\omega},\frac{1}{\omega}\right)^2 - \frac{1-\xi}{2\,\omega}\Phi^{(2)}\!\left(\frac{1}{\omega},\frac{1}{\omega}\right) - \frac{1-\xi}{2}\Omega^{(2)}(1,\omega)\right)\right\} + \mathcal{O}(\alpha_s^3),
\end{aligned}
\tag{30}
$$

$$
\begin{aligned}
C_m^{\text{RI/SMOM}_{\gamma_\mu}}(\omega,\omega) = {}& 1 + \frac{\alpha_s}{4\pi}\,C_F\left(-5 - \frac{\xi}{2} + 3\ln r + \frac{1-\xi}{2}\ln\omega + \frac{1+2\,\omega+(\omega-1)\xi}{2\,\omega}\Phi^{(1)}\!\left(\frac{1}{\omega},\frac{1}{\omega}\right)\right)\\
& + \left(\frac{\alpha_s}{4\pi}\right)^2 C_F\left\{N_c\left(-\frac{8539}{144} - \frac{3\xi}{4} - \frac{\xi^2}{8} + \frac{33-3\xi}{2}\zeta(3) + \frac{151-54\xi-9\xi^2}{72}\ln\omega + \left[\frac{111+\xi^2}{4} + \frac{3\xi^2-13}{12}\ln\omega\right]\ln r\right.\right.\\
& - \frac{13}{4}\ln^2 r + \left[\frac{151+734\,\omega}{72\,\omega} + \frac{2\,\omega-3}{4\,\omega}\xi - \frac{\xi^2}{8\,\omega} - \frac{13+8\,\xi+\xi^2}{8}\ln\omega + \frac{3(1-\omega)\xi^2-13(1+2\,\omega)}{12\,\omega}\ln r\right]\Phi^{(1)}\!\left(\frac{1}{\omega},\frac{1}{\omega}\right)\\
& + \frac{3+6\,\omega+(5\,\omega-2)\xi+(\omega-1)\xi^2}{8\,\omega}\Phi^{(1)}\!\left(\frac{1}{\omega},\frac{1}{\omega}\right)^2 + \frac{\omega}{2}\Phi^{(2)}(1,\omega) - \frac{3+\omega+(\omega-1)\xi}{2\,\omega}\Phi^{(2)}\!\left(\frac{1}{\omega},\frac{1}{\omega}\right) - \frac{1-\xi}{4}\Omega^{(2)}(1,\omega)\\
& \left. + \frac{3-\xi}{8}\Omega^{(2)}\!\left(\frac{1}{\omega},\frac{1}{\omega}\right)\right) + n_f\left(\frac{307}{36} + \ln^2 r - \frac{5}{9}\ln\omega + \frac{\ln\omega-15}{3}\ln r + \frac{(1+2\,\omega)\,(3\ln r-5)}{9\,\omega}\Phi^{(1)}\!\left(\frac{1}{\omega},\frac{1}{\omega}\right)\right)\\
& + \frac{1}{N_c}\left(-\frac{65}{16} - \xi - \frac{\xi^2}{4} - 3(1-\xi)\,\zeta(3) - \frac{9}{4}\ln^2 r + \frac{5-4\xi-\xi^2}{4}\ln\omega + \left[\frac{27}{4} + \frac{3\xi}{4} - \frac{3(1-\xi)}{4}\ln\omega\right]\ln r - \frac{1+\xi}{2}\Omega^{(2)}\,(1,\omega)\right.\\
& + \frac{1}{2}\Omega^{(2)}\!\left(\frac{1}{\omega},\frac{1}{\omega}\right) + \frac{1-\xi+\omega(1+\xi)}{2\omega}\Phi^{(2)}\!\left(\frac{1}{\omega},\frac{1}{\omega}\right) + \left[\frac{-7+2\xi+\xi^2}{8\omega} - \frac{4+5\xi+\xi^2}{8}\right]\Phi^{(1)}\!\left(\frac{1}{\omega},\frac{1}{\omega}\right)^2\\
& \left.\left. + \left[\frac{9+10\xi+3\xi^2}{8} + \frac{5-4\xi-\xi^2}{4\omega} + \frac{3(1-\omega)\xi-3-6\omega}{4\omega}\ln r + \frac{11+8\xi+\xi^2}{8}\ln\omega\right]\Phi^{(1)}\!\left(\frac{1}{\omega},\frac{1}{\omega}\right)\right)\right\} + \mathcal{O}(\alpha_s^3),
\end{aligned}
\tag{31}
$$

where $r = \mu^2/\nu^2$, n_f is the number of quark flavours, and $\Phi^{(2)}$ is given in terms of polylogarithms in [13]. The function $\Psi^{(1)}$ has dropped out of the final results. We do not know the origin of this cancellation, involving many different terms, including the $\mathcal{O}(\epsilon)$ one-loop terms. As an elk test, setting $\mu = \nu$ in (29) and taking $\omega \to 0$, we recover $C_m^{\mathrm{RI'/MOM}}$ [6, 8]. The $\mathcal{O}(\alpha_s)$ terms in (29)–(31) agree with [7] (for $\omega = 1$ and $r = 1$). The most general form $C_m^{\mathrm{RI/SMOM}_{\gamma_\mu}}(\omega, \omega')$, defined in (12), can be obtained from (30) and (31) as

$$C_m^{\mathrm{RI/SMOM}_{\gamma_\mu}}(\omega, \omega') = \frac{C_q^{\mathrm{RI/SMOM}_{\gamma_\mu}}(\omega)}{C_q^{\mathrm{RI/SMOM}_{\gamma_\mu}}(\omega')} C_m^{\mathrm{RI/SMOM}_{\gamma_\mu}}(\omega, \omega).$$

(32)

The mass and field anomalous dimensions in the two schemes are easily obtained by substituting the expressions (29), (30), and (31), as well as $C_q^{\mathrm{SMOM}} = C_q^{\mathrm{RI'/MOM}}$ [6, 8] and the well-known two-loop β-function into (14) and (15). More explicitly, denoting

$$\beta(\alpha_s) = -\beta^{(0)} \left(\frac{\alpha_s}{\pi}\right)^2 - \beta^{(1)} \left(\frac{\alpha_s}{\pi}\right)^3 + \mathcal{O}(\alpha_s^4),$$ (33)

$$C_p^X = 1 + C_p^{X(1)} \left(\frac{\alpha_s}{4\pi}\right) + C_p^{X(2)} \left(\frac{\alpha_s}{4\pi}\right)^2 + \mathcal{O}(\alpha_s^3),$$ (34)

where $p = m$ or $p = q$, $X = \mathrm{RI/SMOM}$ or $\mathrm{RI/SMOM}_{\gamma_\mu}$, $\beta^{(0)} = (11 N_c - 2 n_f)/12$, $\beta^{(1)} = (34 N_c^2 - 10 N_c n_f - 6 C_F n_f)/48$, and the remaining coefficients can be read off (29)–(31), we have to NNLO:

$$\gamma_p^X = \gamma_p^{\overline{\mathrm{MS}}} + 4 \beta^{(0)} C_p^{X(1)} \left(\frac{\alpha_s}{4\pi}\right)^2$$
$$+ 4 \left\{ \beta^{(0)} \left[2 C_p^{X(2)} - \left(C_p^{X(1)}\right)^2 \right] + 4 \beta^{(1)} C_p^{X(1)} \right\} \left(\frac{\alpha_s}{4\pi}\right)^3$$
$$+ \Delta_p^X + \mathcal{O}(\alpha_s^4).$$ (35)

Here

$$\Delta_p^X \equiv \delta(\alpha_s, \xi) \left[C_p^X \right]^{-1} \frac{\partial C_p^X}{\partial \xi},$$ (36)

which vanishes in the Landau gauge, is again straightforward to evaluate to $\mathcal{O}(\alpha_s^3)$ from (29)–(31) and the perturbation expansion of δ defined in (16). Gauge invariance implies $\delta = \gamma_A \xi$, where γ_A is the anomalous dimension of the gluon field (defined analogously to (16)) [21–23], giving

$$\delta = \frac{\alpha_s}{4\pi} \xi \left(\frac{13 - 3\xi}{6} N_c - \frac{2}{3} n_f \right)$$
$$+ \left(\frac{\alpha_s}{4\pi}\right)^2 \xi \left(\frac{59 - 11\xi - 2\xi^2}{8} N_c^2 - \frac{7 N_c^2 - 2}{2 N_c} n_f \right) + \mathcal{O}(\alpha_s^3).$$ (37)

PHENOMENOLOGY

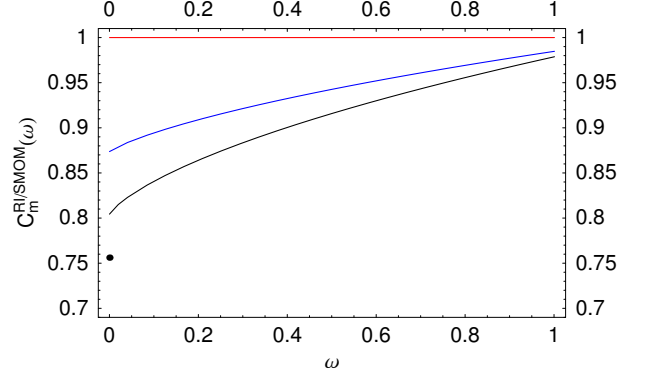To explore the phenomenological consequences of our result for QCD with three dynamical light quarks (as in

FIG. 3. Conversion factors $C_m^{\mathrm{RI/SMOM}}$ as function of $\omega = q^2/p^2$ at LO (top/red), NLO (middle/blue), and NNLO (bottom/black), and $C_m^{\mathrm{RI'/MOM}} = C_m^{\mathrm{RI/SMOM}}(0)$ at NNNLO (dot).
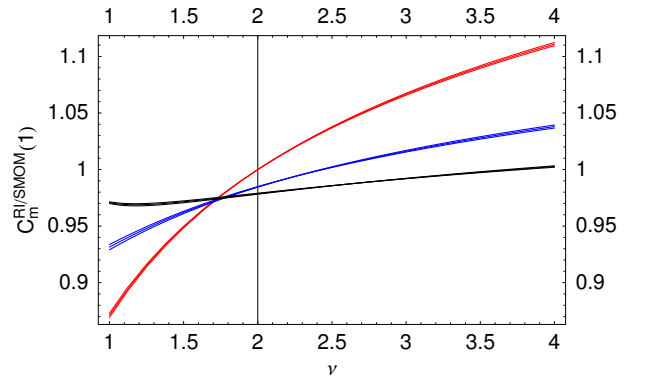

FIG. 4. Residual matching-scale dependence of the conversion factor $C_m^{\mathrm{RI/SMOM}}$ at $\omega = 1$ at LO (red), NLO (blue), and NNLO (black).

nature, and in modern unquenched simulations), we set $n_f = 3$. Figure 3 shows the conversion factor $C_m(\omega)$ in the Landau gauge. We observe that the NNLO correction, like the NLO term, is very small at the SMOM point $\omega = 1$. This is in contrast to the RI'/MOM scheme $\omega = 0$, where even the next-to-next-to-next-to-leading-order (NNNLO) correction [6, 8] is large (dot in the Figure). To estimate the effects from uncomputed $\mathcal{O}(\alpha_s^4)$ terms, we vary the renormalization scale (matching scale) ν used in the conversion and evolve $C_m^{\mathrm{RI/SMOM}}(\omega = 1; \nu)$ to the fixed scale $\mu = 2$ GeV, which gives a formally ν-independent number [19, 20]. The result is shown in Figure 4. The width of each band, due to the uncertainty on $\alpha_s(M_Z) = 0.1184 \pm 0.0007$ [18], is almost negligible. This is a consequence of the smallness of the NLO and NNLO corrections. We observe that the NNLO result is almost scale-independent. Alternatively, we can convert the $\overline{\mathrm{MS}}$ mass to the RGI quark mass employing the relevant expressions in [20], which is also scale-independent. The result is similarly stable under scale variation, but the α_s dependence is a bit more pronounced. A slightly larger

residual scale dependence is found for the RI/SMOM$_{\gamma_\mu}$ scheme. Numerically, we obtain

$$m^{\overline{\mathrm{MS}}}(2\,\mathrm{GeV})$$
$$= \left(0.979^{+0.024}_{-0.010}\big|_{\mathrm{h.o.}}{}^{+0.001}_{-0.001}\big|_{\alpha_s}\right) m^{\mathrm{RI/SMOM}}(2\,\mathrm{GeV}),$$
$$= \left(0.932^{+0.030}_{-0.021}\big|_{\mathrm{h.o.}}{}^{+0.003}_{-0.003}\big|_{\alpha_s}\right) m^{\mathrm{RI/SMOM}_{\gamma_\mu}}(2\,\mathrm{GeV}),$$
$$m^{\mathrm{RGI}} = \left(2.53^{+0.05}_{-0.02}\big|_{\mathrm{h.o.}}{}^{+0.02}_{-0.02}\big|_{\alpha_s}\right) m^{\mathrm{RI/SMOM}}(2\,\mathrm{GeV})$$
$$= \left(2.41^{+0.07}_{-0.04}\big|_{\mathrm{h.o.}}{}^{+0.03}_{-0.03}\big|_{\alpha_s}\right) m^{\mathrm{RI/SMOM}_{\gamma_\mu}}(2\,\mathrm{GeV}),$$

corresponding to a perturbative uncertainty of less than 2%, or about 2 MeV for the strange quark mass, when converting from the RI/SMOM scheme, and about 3% for the RI/SMOM$_{\gamma_\mu}$ scheme. As also the absolute size of the NLO and NNLO corrections is larger for the RI/SMOM$_{\gamma_\mu}$ scheme, we advocate the use of the RI/SMOM scheme together with an appropriate error estimate in extracting results for the light quark masses.

CONCLUSION

We have computed the RI/SMOM $\to$ $\overline{\mathrm{MS}}$ and RI/SMOM$_{\gamma_\mu}$ $\to$ $\overline{\mathrm{MS}}$ conversion factors for the quark mass to NNLO and shown that the RI/SMOM and RI/SMOM$_{\gamma_\mu}$ schemes, designed to reduce sensitivity to low-energy non-perturbative physics, are perturbatively very well behaved, too. These schemes thus may be used to extract quark masses with percent-level accuracy from numerical lattice QCD. An important question is whether the same holds true for other quantities of interest, such as B_K and other hadronic matrix elements.

We are happy to thank Chris Sachrajda for a talk and conversations raising our interest in the topic and him and Andrzej Buras for comments on the manuscript. M. G. thanks the Galileo Galilei institute for hospitality and the INFN for support during a stay.

Note: After the initial submission of this manuscript to the Arxiv, Ref. [24] appeared, whose authors compute the conversion factor C_m at NNLO for the symmetric renormalization point $\omega = 1$, where they confirm our result. They also give the corresponding field and mass conversion factors $C_q^{\mathrm{RI/SMOM}_{\gamma_\mu}}$ and $C_m^{\mathrm{RI/SMOM}_{\gamma_\mu}}$ for the RI/SMOM$_{\gamma_\mu}$ scheme, as well as expressions for the NNLO anomalous dimensions in both schemes. In this revised version, we have given expressions for those quantities, as well. Specialising to $\omega = \omega' = r = 1$, our results for the C_q^X agree with the results in [24]. Setting

further $\xi = 0$, we agree with the results for γ_q^X given there, up to a global sign difference [25].

————

* martin.gorbahn@ph.tum.de
† S.Jaeger@sussex.ac.uk
[1] See e.g. C.T. Sachrajda, arXiv:0911.1560 [hep-lat]; V. Lubicz, PoS **LAT2009**, 013 (2009).
[2] G. Martinelli, C. Pittori, C.T. Sachrajda, M. Testa and A. Vladikas, Nucl. Phys. B **445**, 81 (1995).
[3] K. Jansen *et al.*, Phys. Lett. B **372**, 275 (1996); S. Capitani, M. Guagnelli, M. Luescher, S. Sint, R. Sommer, P. Weisz and H. Wittig, Nucl. Phys. Proc. Suppl. **63**, 153 (1998).
[4] W. A. Bardeen, A. J. Buras, D. W. Duke and T. Muta, Phys. Rev. D **18**, 3998 (1978).
[5] Y. Aoki *et al.*, Phys. Rev. D **78**, 054510 (2008).
[6] K. G. Chetyrkin and A. Retey, Nucl. Phys. B **583**, 3 (2000).
[7] C. Sturm, Y. Aoki, N.H. Christ, T. Izubuchi, C.T. Sachrajda and A. Soni, Phys. Rev. D **80**, 014501 (2009).
[8] J.A. Gracey, Nucl. Phys. B **662**, 247 (2003).
[9] R. Tarrach, Nucl. Phys. B **183**, 384 (1981).
[10] O. V. Tarasov, JINR P2-82-900 (unpublished).
[11] K. G. Chetyrkin, Phys. Lett. B **404** (1997) 161 [arXiv:hep-ph/9703278].
[12] J. A. M. Vermaseren, S. A. Larin and T. van Ritbergen, Phys. Lett. B **405** (1997) 327 [arXiv:hep-ph/9703284].
[13] N.I. Usyukina and A.I. Davydychev, Phys. Lett. B **332**, 159 (1994).
[14] N.I. Usyukina and A.I. Davydychev, Phys. Lett. B **348**, 503 (1995).
[15] A.V. Smirnov, JHEP **0810**, 107 (2008).
[16] S. Laporta, Int. J. Mod. Phys. A **15**, 5087 (2000).
[17] A.V. Smirnov and V.A. Smirnov, JHEP **0601**, 001 (2006). A.V. Smirnov and V.A. Smirnov, Nucl. Phys. Proc. Suppl. **160**, 80 (2006).
[18] S. Bethke, Eur. Phys. J. C **64**, 689 (2009).
[19] We use the program RunDec for the running of α_s at the appropriate order and for decoupling heavy quarks at their thresholds. The program is described in Ref. [20].
[20] K.G. Chetyrkin, J.H. Kuhn and M. Steinhauser, Comput. Phys. Commun. **133**, 43 (2000)
[21] O. V. Tarasov and A. A. Vladimirov, Sov. J. Nucl. Phys. **25** (1977) 585 [Yad. Fiz. **25** (1977) 1104].
[22] S. A. Larin and J. A. M. Vermaseren, Phys. Lett. B **303**, 334 (1993) [arXiv:hep-ph/9302208].
[23] K. G. Chetyrkin, Nucl. Phys. B **710**, 499 (2005) [arXiv:hep-ph/0405193].
[24] L. G. Almeida and C. Sturm, arXiv:1004.4613 [hep-ph].
[25] We thank the authors of [24] for correspondence in which they informed us that this disagreement is due to a typo in that paper.